

## LETTER

# Runaway electrons generated during spontaneous disruptions in the EAST tokamak

To cite this article: R.J. Zhou *et al* 2017 *Nucl. Fusion* **57** 114002

View the [article online](#) for updates and enhancements.

## You may also like

- [Design of far-infrared polarimeter/interferometer system for EAST tokamak](#)  
H Q Liu, Y X Jie, W X Ding et al.
- [Characterization of disruption halo current between 'W-Like' graphite divertor and 'ITER-Like' divertor structure on EAST tokamak](#)  
D L Chen, R S Granetz, L Zeng et al.
- [Hybrid deep-learning architecture for general disruption prediction across multiple tokamaks](#)  
J.X. Zhu, C. Rea, K. Montes et al.

## Letter

# Runaway electrons generated during spontaneous disruptions in the EAST tokamak

R.J. Zhou, L.Q. Hu, Y. Zhang, G.Q. Zhong, S.Y. Lin and The EAST Team<sup>a</sup>

Institute of Plasma Physics, Chinese Academy of Sciences, Hefei 230031, People's Republic of China

E-mail: [lqhu@ipp.ac.cn](mailto:lqhu@ipp.ac.cn)

Received 4 April 2017, revised 6 June 2017

Accepted for publication 29 June 2017

Published 3 August 2017

**Abstract**

The runaway electrons produced during spontaneous disruptions were studied when lower hybrid wave heating was used in the EAST tokamak. Up to 60% of the pre-disruptive plasma current can be transferred to runaway current in the disruptions when seed fast electrons exist in the plasma. The evolutions of the radial profile of the electric field and the runaway electron density are obtained with the aid of an one-dimensional self-consistent simulation model. The results clearly show the competition between the radial diffusion of the induced electric field and growth of the runaway current. They also indicate that the dominant runaway generation mechanism was of Dreicer type, and half of the decreasing magnetic energy was converted into runaway electron kinetic energy during the disruptions.

Keywords: runaway electrons, disruptions, EAST

(Some figures may appear in colour only in the online journal)

Plasma disruption is one of the most dangerous events in large tokamaks and it is also one of the problems that need to be solved urgently. Among all of the types of deleterious effects during disruption, the production of runaway electrons (REs) can be a very serious issue [1, 2]. In present-day tokamaks, most of the disruptions occurring spontaneously in experiments do not generate significant runaway tails during current quench. In contrast, due to the large plasma magnetic energy, large electric field during current quench and the longer duration of the current quench itself, significant runaway currents are expected to be routinely generated during disruptions in the next-generation devices such as ITER [3–6]. To study the dynamics of REs during disruptions, dedicated experiments have been set up to trigger disruptions that are intended to produce large runaway current plateaus, in which injection of a large amount of inert gases is usually involved [7–9]. Obviously, when a large amount of inert gas exists in plasma

already, the dynamics of RE generation can be very different from the situation in spontaneous disruptions. The study of runaway electron generation during spontaneous disruptions in experiments is important for understanding the nature of disruption-generated runaways.

In the EAST tokamak, usually the disruptions occurring spontaneously in experiments do not generate runaway tails during the current quench. This is mainly due to the small toroidal electric fields induced because of the small plasma current and slow current decay during current quenches. Recently, the production of REs during spontaneous disruptions in the EAST tokamak has been observed in experiments when lower hybrid wave (LHW) heating was used during disruptions.

EAST is a fully superconducting tokamak with a major radius  $R = 1.7\text{--}1.9$  m, minor radius  $a = 0.4\text{--}0.45$  m, maximum plasma current  $I_p = 1$  MA and maximum toroidal field  $B_t = 3.5$  T. The LHW system, with a maximum injection power of 4 MW at 2.45 GHz, is one of the most reliable heating and current drive systems in EAST [10].

<sup>a</sup> See the appendix of Wan *et al* [10].

Shown in figure 1 is a typical discharge in which a runaway current plateau was produced during spontaneous disruption when LHW heating was used. The sudden decrease of the electron cyclotron emission (ECE) indicates the occurrence of thermal quench, followed by the current quench phase after less than 1 ms. Then, the loop voltage started to increase, and a loss of REs was observed. The position of the plasma was shifted to the low field side.

During the current quench phase, a runaway plateau developed after about 10 ms. The injected LHW, with power of about 350 kW, provided seed fast electrons which could easily be transferred to REs when the loop voltage was increasing. About 60% of the pre-disruptive plasma current was transferred to runaway current. The arising runaway current prevented the plasma current from dropping to a very low value under which the plasma control would go into the protection procedure. The increasing runaway current gradually replaced the plasma current, which is indicated by the increase of ECE emission. The plasma current even increased slightly during the runaway plateau. As a response, loop voltage decreased right after the development of the runaway plateau. The position of the plasma was also shifted back. The plasma was very stable during the runaway plateau phase, except for a sudden plasma shift at about 3.6 s. This sudden plasma shift caused enhanced loss of REs and seed fast electrons, which was evidenced by the spikes in the flux of lost REs, hard x-ray (HXR) and ECE signals.

The runaway plateau lasted for about 110 ms, followed by the terminal phase which lasted for about 100 ms. During the runaway terminal phase, loop voltage increased and ECE emission decreased, accompanied by the emergence of magnetic fluctuations in Mirnov and saddle coil signals. In more detail, the loss characteristics of REs were related to the characteristics of magnetic fluctuations. From the flux of lost REs and HXR signals, the loss of REs was ‘bursty’, which has also been found in other devices [11, 12]. The flux of lost REs was monitored through their thick-target bremsstrahlung emission, HXR is the flux of HXRs, and VB is the visible bremsstrahlung emission from plasma impurity. To achieve a higher time resolution comparing to the energy spectrum, the ‘flux’ data here are obtained by sending the signals from amplifiers into the integrators to integrate the counts and energy of x-rays.

The dynamics of the spontaneous disruption runaways in EAST is studied with the aid of an one-dimensional self-consistent simulation model, in which the diffusion of the induced electric field in the plasma and the generation and loss mechanisms of REs during disruption are coupled together [13–15]. Considering the experimental results from EAST, the existence of seed fast electrons is an important condition to produce disruption runaways. Therefore, a source term is also included in the model. The dynamics of REs based on the test particle model in momentum space will be also coupled to this model in the near future to monitor the evolution of runaway energy.

In the model, evolution of the induced electric field in cylindrical geometry is governed by

$$\mu_0 \frac{\partial}{\partial t} (\sigma_{\parallel} E_{\parallel} + j_r) = \frac{1}{r} \frac{\partial}{\partial r} r \frac{\partial E_{\parallel}}{\partial r}, \quad (1)$$

in which  $\mu_0$  is the vacuum permeability,  $\sigma_{\parallel}$  is the neoclassical conductivity,  $E_{\parallel}$  is the induced parallel electric field during disruption and  $j_r$  is the current density carried by REs.

Evolution of runaway current is governed by primary (‘Dreicer’) and secondary (‘avalanche’) runaway generation processes, the diffusion loss mechanism and the source of seed runaways:

$$\frac{\partial j_r}{\partial t} = \text{ecn}_e \nu(v_r) \lambda + \frac{j_r}{\tau_s} + \frac{1}{r} \frac{\partial}{\partial r} r D_r \frac{\partial j_r}{\partial r} + S, \quad (2)$$

in which

$$\lambda = \lambda_{\text{nonrel}} \exp\left\{-\frac{T_e}{m_e c^2} \left[\frac{\varepsilon^2}{8} + \frac{2\varepsilon^{3/2}}{3} (1 + Z_{\text{eff}}^{1/2})\right]\right\}, \quad (3)$$

$$\lambda_{\text{nonrel}} = K(Z_{\text{eff}}) \varepsilon^{-3(1+Z_{\text{eff}})/16} \exp\left(-\frac{1}{4\varepsilon} - \sqrt{\frac{1+Z_{\text{eff}}}{\varepsilon}}\right), \quad (4)$$

$$\begin{aligned} \frac{1}{\tau_s} &= \frac{1}{\tau \ln \Lambda} \sqrt{\frac{\pi \varphi}{3(Z_{\text{eff}} + 5)}} \left(\frac{E_{\parallel}}{E_c} - 1\right) \\ &\times \left(1 - \frac{E_c}{E_{\parallel}} + \frac{4\pi(Z_{\text{eff}} + 1)^2}{3\varphi(Z_{\text{eff}} + 5)(E_{\parallel}^2/E_c^2 + 4/\varphi^2 - 1)}\right)^{-1/2}, \end{aligned} \quad (5)$$

$$\tau = \frac{1}{\nu(v_r)} = \frac{4\pi \varepsilon_0^2 m_e^2 v_r^3}{e^4 n_e \ln \Lambda}. \quad (6)$$

$K(Z_{\text{eff}})$  is a weak function of  $Z_{\text{eff}}$  [16];  $\varepsilon_0$  is the vacuum permittivity;  $\ln \Lambda$  is the Coulomb logarithm;  $\varepsilon = E_{\parallel}/E_D$ , with Dreicer field  $E_D = e^3 n_e \ln \Lambda / 4\pi \varepsilon_0^2 T_e$ , and critical electric field  $E_c = e^3 n_e \ln \Lambda / 4\pi \varepsilon_0^2 m_e c^2$ ;  $\varphi = 1 - 1.46(r/R)^{1/2} + 1.72r/R$  describes the effect of finite aspect ratio [17];  $\tau$  is the electron collision time during the Dreicer process in which only small deflections of the velocity vector (small angle Coulomb collision) result; and  $\tau_s$  is the collision time during the avalanche process in which the velocities of the colliding particles change appreciably (large angle Coulomb collision) [13].  $1/\tau$  and  $1/\tau_s \approx 1/(\tau \ln \Lambda)$  (the detailed expression is shown in equation (5)) represent the frequency of small angle Coulomb collision and large angle Coulomb collision, respectively. Diffusion loss of REs is considered to be governed by magnetic fluctuations [18, 19], with runaway diffusion coefficient  $D_r = \Upsilon \pi q v_{\parallel} R \tilde{b}^2$  [20]. The factor  $\Upsilon$ , known as a shielding factor, describes the deviation of the RE diffusion from the thermal electron diffusion due to the displacement of the RE orbits from the magnetic surfaces (orbit-averaging) and their large gyro-radii (gyro-averaging).  $S$  is a source term that provides seed REs, the value of which in first order approximation is proportional to the injected LHW power and plasma density.

The evolution of electron temperature during thermal quench and current quench phases is governed by:

$$T_e(x, t) = T_1(x) + [T_0(x) - T_1(x)] e^{-t/t_0}, \quad (7)$$

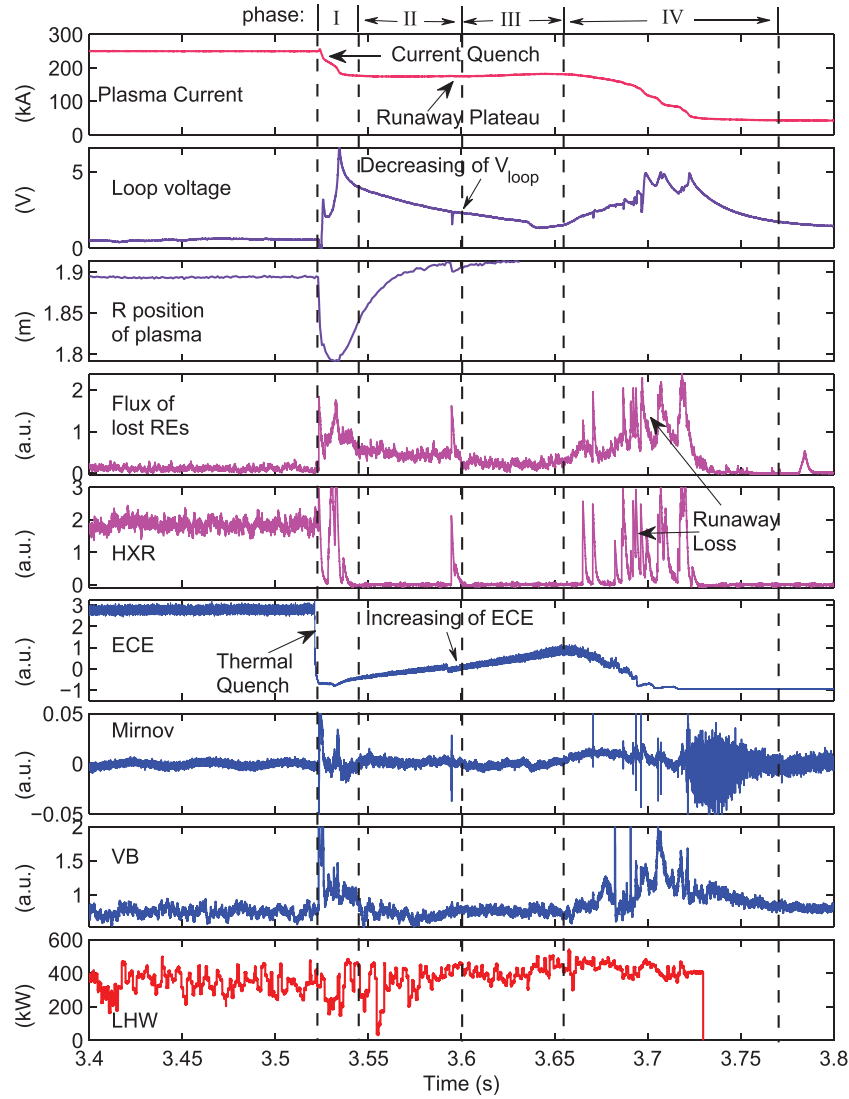


**Figure 1.** One typical discharge in which a runaway current plateau was produced during spontaneous disruption.

in which  $x = r/a$  is the normalized plasma radius,  $T_0(x) = T_0(0)(1 - 0.9x^2)^2$ , and  $T_1(x) = T_1(0)(1 - 0.9x^2)$ .  $T_0(0)$  is the central electron temperature just before thermal quench, and  $T_1(0)$  is the central electron temperature long after the current quench.  $t_0$  represents the thermal quench time scale. The electron temperature profile will be less and less peaking during the evolution of the disruption, which is consistent with the experimental conditions. The evolution of plasma density is governed by:

$$n_e(x, t) = n_{e0}(t)(1 - 0.9x^2)^{1/2}, \quad (8)$$

in which  $n_{e0}(t)$  is the central plasma density [14].

All available experimental data are used as the input of the model. For example, the values of  $Z_{\text{eff}}$  (reconstructed by the visible bremsstrahlung measurement system),  $n_{e0}$  (calculated by the hydrogen cyanide (HCN) interferometer system),  $T_0(0)$  (calculated by the soft x-ray pulse height analysis (PHA) system),  $t_0$  (deduced from ECE signals), and  $D_r$  (calculated from the Mirnov and flux of lost RE signals), etc.  $I_p$  is from the experimental data and is used as a reference parameter, while  $V_{\text{loop}}$

is from experimental data and is used as a boundary condition for the electric field. The effect of the electric field induced by Ohmic coils is also included,  $E_{\parallel} = E_{\text{Ohmic coils}} + E_{dI_p/dt}$ , because  $E_{\text{Ohmic coils}}$  is not negligibly small, in particular in the edge region of the plasma, which can be seen from the experimental data (e.g. at the end of the discharge after 3.75 s in figure 1).

The start time of the model is at the beginning of thermal quench of the discharge. The evolution of electric field, RE density and currents is shown in figures 2–4, respectively. The whole evolution can be divided into four phases based on its nature:

1. During the current quench phase (1–25 ms), the radial profile of the electric field was hollow due to the fact that REs were initially produced more effectively in the center of the plasma, which can be seen from figure 2(a). Plasma current would decrease more slowly in the center, which would make the induced electric field lower there. Seen from figure 2(b), the value of  $E$  was higher around the radial range  $r/a \sim 0.5$ , and its values in the edge and

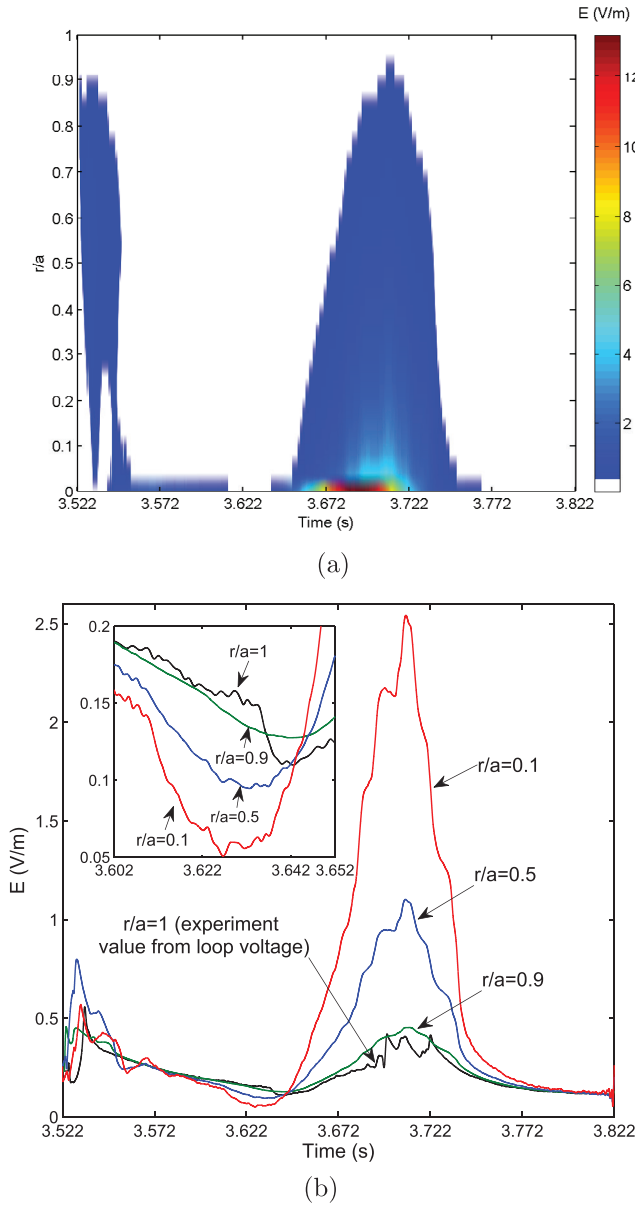


**Figure 2.** Time evolution of electric field. (a) In this radial profile evolution, the color for electric field value lower than  $0.5 \text{ V m}^{-1}$  was deleted to distinguish the evolution characteristics of the electric field. (b) Evolution of the electric field in four radial positions:  $r/a = 0.1, 0.5, 0.9$ , and  $1$ , in which the value of the electric field at  $r/a = 1$  is the experimental value from the loop voltage.

center were about the same. Then the electric field was diffused into the center of the plasma. This behavior of  $E$  evolution has also been mentioned in [14].

- During the runaway plateau phase 1 (25–75 ms), the electric field was more uniform along the radial direction. In this phase, the radial profile of REs was stable (seen from figure 3), and almost all plasma current was already carried out by runaway current (seen from figure 4(a)).
- During the runaway plateau phase 2 (75–130 ms), REs were produced more significantly in the center of the plasma (seen from figure 3), which made the electric field in the center lower than the edge value (see figure 2(b)).

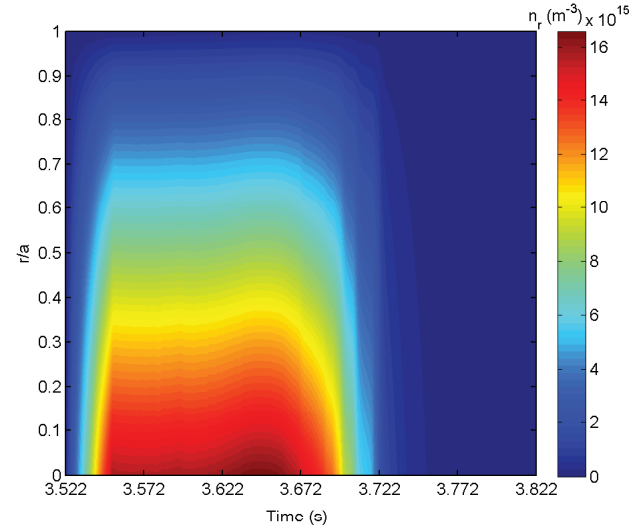


**Figure 3.** Time and radial profile evolution of RE density. Runaway electrons were produced mainly in the center region of the plasma. In the center region, the maximum runaway growth rate was at the initial phase of the disruption, and this region had the maximum runaway loss rate in the end phase of the disruption as well.

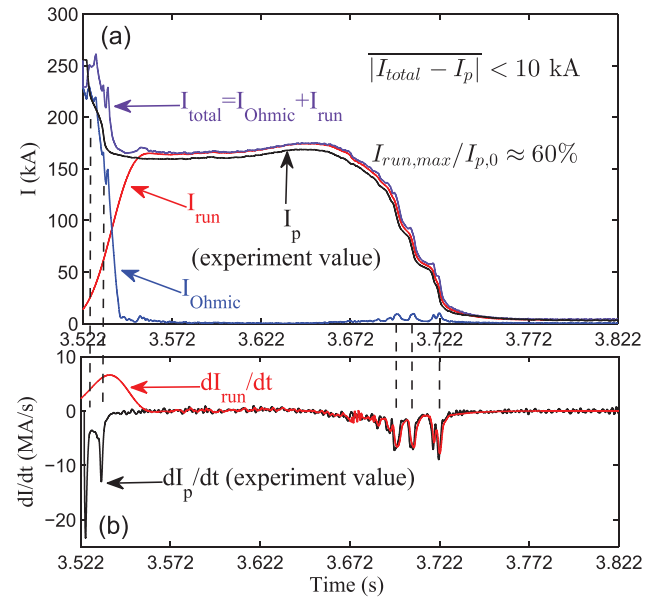


**Figure 4.** (a) Time evolution of runaway current, Ohmic current and total current from a simulation in zero radial dimensional (integrated from one-dimensional results), and plasma current from the experimental value. (b) Current change rate of the plasma current from the experimental value and runaway current.

In fact, the value of the electric field during this phase was the lowest in the whole time period, even lower than the value in the end time points (250–300 ms).  $E_{\text{Ohmic}}$  coils kept almost the same in the whole time period, which can be seen from the evolution of the current of all Ohmic coils. Therefore, considering the relation  $E_{\parallel} = E_{\text{Ohmic coils}} + E_{dI_p/dt}$ , the plasma current during this phase was increasing, at least in the center region. The fact that the plasma current even increased slightly during the runaway plateau (seen from figure 1) could be evidence for this phenomenon.



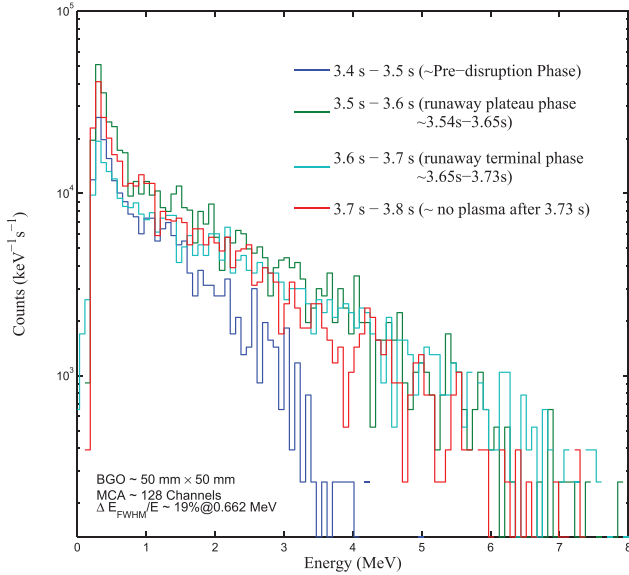


**Figure 5.** Energy spectra of thick-target bremsstrahlung emission from lost REs from 3.4 s to 3.9 s. Detector type: BGO scintillator (50 mm × 50 mm); spectra time resolution: 100 ms; multi-channel analyzer (MCA) resolution: 128; spectra energy resolution:  $\Delta E_{\text{FWHM}}/E \sim 19\%$  @ 0.662 MeV, in which FWHM means full width at half maximum.

4. During the runaway terminal phase (130–250 ms), plasma current started to decrease again, and a strong electric field was also induced again. Different from phase 1, almost all of the current was carried out by REs in this phase (seen from figure 4(a)), and the runaway current is highly peaked in the center. So, the loss of REs induced a strong electric field in the center of the plasma, and the electric field was diffused from the center to the edge (see figures 2(a) and (b)). Ohmic current was also increased due to the strong induced electric field (see figure 4). The electron temperature in this phase was very low, so this strong electric field only produced a very small Ohmic current.

As seen from figure 4 in zero-dimensional evolution of the currents, the value of the electric field was mainly proportional to the change rate of the plasma current  $dI_p/dt$ . The runaway current growth rate  $dI_{\text{run}}/dt$  was increased smoothly when the electric field was strong, then decreased to zero, and remained around zero when the electric field was very low. However,  $dI_p/dt$  did not evolve smoothly like  $dI_{\text{run}}/dt$ . Considering the fact that the Dreicer runaway generation rate has an exponential relationship with the electric field (see equation (4)), and the avalanche runaway generation rate has a linear relationship with the electric field (see equation (5)) [13, 17, 21, 22], the dominant runaway generation mechanism here should be the Dreicer type.

The energy of lost REs was monitored through their thick-target bremsstrahlung emission, which was measured by a set of bismuth germanate (BGO) scintillator detectors [23]. The system can deal with a count-rate up to about 200 kHz with a pile-up rejection function, while the count-rate in this

discharge was no higher than 40 kHz. The energy spectrum of the thick-target bremsstrahlung emission is a continuous spectrum with the relation  $E_{\text{thick}} \leq E_{\text{REs}} - m_e c^2$ . So the maximum energy in the energy spectrum is  $E_{\text{thick}}^{\text{max}} = E_{\text{REs}} - m_e c^2$ . Therefore the increase of  $E_{\text{thick}}^{\text{max}}$  can represent the increase of RE energy. The energy spectra of thick-target bremsstrahlung emission caused by lost REs from 3.4 s to 3.9 s is shown in figure 5 with a time resolution of 100 ms. It can be seen that the maximum energy of the thick-target bremsstrahlung emission increased from 4 MeV to 7 MeV after the disruption, which indicated that the energy of REs increased 3 MeV. This can be understood if half of the decreasing magnetic energy is converted into RE kinetic energy [3, 24]. REs were accelerated by the induced electric field during disruption, and the induced electric field was created due to the decrease of magnetic flux. During the disruption, the decrease of magnetic energy was  $\Delta E_{\text{mag}} = \Delta(L_p I_p^2/2) \approx 75$  kJ as a rough estimation, in which  $L_p = \mu_0 R_0 (\ln(8R_0/a) - 2 + I_i/2)$  is the total plasma inductance. Integrated from figure 3, the average runaway density is about  $\bar{n}_r \approx 1 \times 10^{16} \text{ m}^{-3}$ . Assuming that half of the decreasing magnetic energy was transferred to runaway energy, the average runaway energy can be expected to increase by about 3 MeV, which is consistent with the experimental results.

In summary, the REs produced during spontaneous disruptions are studied when LHW heating was used in the EAST tokamak. Up to 60% of the pre-disruptive plasma current was transferred to runaway current with a runaway plateau that lasted for about 110 ms. It represents a typical feature of the spontaneous disruptions when seed fast electrons exist in the plasma.

With the aid of an one-dimensional self-consistent simulation model—in which the diffusion of induced electric field, generation and loss mechanisms of REs, and source term of seed fast electrons during disruptions are coupled together with all available experiment data as the input parameters—the evolution of radial profiles of the electric field and RE density are obtained. Both the experimental and simulation results clearly show competition between the radial diffusion of the induced electric field and growth of runaway current. It also indicates that the dominant runaway generation mechanism was of Dreicer type, and half of the decreasing magnetic energy was converted into RE kinetic energy during the disruptions.

## Acknowledgments

One of the authors (R.J. Zhou) would like to thank Professor K. Toi (NIFS, Japan), and Professor Q. Yu (Max-Planck-Institut (MPI), Germany) for helpful discussions on the experimental results. This work was supported by the National Nature Science Foundation of China under Grant No. 11405219 and was partially supported by the JSPS-NRF-NSFC A3 Foresight Program in the field of Plasma Physics (NSFC No. 11261140328).

## References

- [1] Mirnov S., Wesley J., Fujisawa N., Gribov Y., Gruber O., Hender T., Ivanov N., Jardin S., Lister J. and Perkins F. 1999 *Nucl. Fusion* **39** 2251
- [2] Hender T., Wesley J., Bialek J., Bondeson A., Boozer A., Buttery R., Garofalo A., Goodman T., Granetz R. and Gribov Y. 2007 *Nucl. Fusion* **47** S128
- [3] Loarte A., Riccardo V., Martin-Sols J., Paley J., Huber A., Lehnen M. and JET Contributors 2011 *Nucl. Fusion* **51** 073004
- [4] Martin-Sols J., Loarte A., Hollmann E., Esposito B., Riccardo V., Teams D.D. and JET Contributors 2014 *Nucl. Fusion* **54** 083027
- [5] Hollmann E.M. et al 2015 *Phys. Plasmas* **22** 021802
- [6] Granetz R.S. et al 2014 *Phys. Plasmas* **21** 072506
- [7] Lehnen M. et al 2013 *Nucl. Fusion* **53** 093007
- [8] Lehnen M., Abdullaev S., Arnoux G., Bozhnikov S., Jakubowski M., Jaspers R., Plyusnin V., Riccardo V. and Samm U. 2009 *J. Nucl. Mater.* **390** 740
- [9] Plyusnin V., Riccardo V., Jaspers R., Alper B., Kiptily V., Mlynar J., Popovichev S., de La Luna E. and Andersson F. 2006 *Nucl. Fusion* **46** 277
- [10] Wan B., Li J., Guo H., Liang Y., Xu G., Wang L. and Gong X. 2015 *Nucl. Fusion* **55** 104015
- [11] Gill R. 1993 *Nucl. Fusion* **33** 1613
- [12] Gill R., Alper B., Edwards A., Ingesson L., Johnson M. and Ward D. 2000 *Nucl. Fusion* **40** 163
- [13] Helander P., Eriksson L.G. and Andersson F. 2002 *Plasma Phys. Control. Fusion* **44** B247
- [14] Eriksson L., Helander P., Andersson F., Anderson D. and Lisak M. 2004 *Phys. Rev. Lett.* **92** 205004
- [15] Eriksson L. and Helander P. 2003 *Comput. Phys. Commun.* **154** 175
- [16] Jaspers R. 1995 Relativistic runaway electrons in tokamak plasmas *PhD Thesis* Technical University of Eindhoven
- [17] Rosenbluth M. and Putvinski S. 1997 *Nucl. Fusion* **37** 1355
- [18] Helander P., Eriksson L.G. and Andersson F. 2000 *Phys. Plasmas* **7** 4106
- [19] Martin-Solis J.R., Sanchez R. and Esposito B. 1999 *Phys. Plasmas* **6** 3925
- [20] Zhou R.J., Hu L.Q., Li E.Z., Xu M., Zhong G.Q., Xu L.Q. and Lin S.Y. 2013 *Phys. Plasmas* **20** 032511
- [21] Dreicer H. 1959 *Phys. Rev.* **115** 238
- [22] Dreicer H. 1960 *Phys. Rev.* **117** 329
- [23] Zhou R.J., Hu L.Q., Zhong G.Q., Cao H.R., Liu G.Z., Li K., Zhang Y., Lin S.Y., Zhang J.Z. and Team E. 2016 *Rev. Sci. Instrum.* **87** 11E702
- [24] Riemann J., Smith H. and Helander P. 2012 *Phys. Plasmas* **19** 012507